

## Approximate Cone-Beam Filtered Backprojection for Limited Angle Tomography

Seungjun Yoo<sup>a</sup>, Ho Kyung Kim<sup>a,b,\*</sup>

<sup>a</sup> School of Mechanical Engineering, Pusan Nat'l Univ., Busandaehakro 63beon-gil, Busan 46241

<sup>b</sup> Center for Advanced Medical Engineering Research, Pusan Nat'l Univ., Busandaehakro 63beon-gil, Busan 46241

\*Corresponding author: hokyung@pusan.ac.kr

### 1. Introduction

The limited-angle tomography is one in which the data collection does not span the full range of projection angles needed for accurate computed tomography (CT) image reconstruction. This situation frequently meets in industrial non-destructive testing applications [1,2]. Since the incomplete data collection results in the null space in the Fourier space, also known as the missing cones, the conventional filtered backprojection (FBP) method causes artifacts in the reconstructed images [3]. Unfortunately, no linear filtering can recover the missing Fourier data at all. Extrapolating the measured Fourier data into the missing region may be another approach, but it would be sensitive to noise, hence useless in practice. The use of a priori knowledge of the object in the reconstruction may offer estimates in the null space [4], but it is challenging to quantify how effective the prior knowledge can be in compensating for missing data.

The authors pay attention to the development of ectomography based on the shift-and-add method for circular tomosynthesis trajectory [5]. Ectomography truncates the Fourier data deliberately and reduces the fractional missing region, hence reducing the artifact, while sacrificing the depth resolution. In this study, we extend the concept of ectomography to the cone-beam (CB) filtered backprojection (FBP) method or the Feldkamp algorithm [6] in an isocentric circular trajectory. We introduce a low-pass filter along the depth direction to the Feldkamp algorithm, which plays a similar role as the ectomized slices in ectomography.

### 2. Methods and Materials

#### 2.1 Approximate FBP for Limited-Angle Tomography

Given the filtered projections  $g_{\beta}^*(u, v)$ , where  $(u, v)$  refers to the detector coordinates, obtained over a scanning angular range  $\beta_{\text{scan}}$  in an isocentric orbit, the slice image  $f(x, y)$  at a depth  $z$  can be given by

$$f(x, y; z) = k \int_{\beta_{\text{scan}}} \frac{D^2}{(d-l)^2} g_{\beta}^*(u, v) d\beta, \quad (1)$$

where  $k$  represents the normalization factor. There are three different distance parameters from the source to the axis of rotation  $d$ , the detector  $D$ , and the reconstruction plane  $l$ . On the other hand, the filtered projection is obtained from the convolution integration between the weighted projection and the convolution kernel  $h$ :

$$g_{\beta}^*(u, v) = \int_{-\infty}^{\infty} \left[ \frac{D^2}{\sqrt{D^2+u^2+v^2}} g_{\beta}(u, v) \right] h\left(\frac{Dx'}{d-l} - u\right) d\beta, \quad (2)$$

where  $x'$  indicates the x-axis rotated by an amount of the projection angle  $\beta$ .

This FBP can be analyzed equivalently in the backprojection-then-filtering domain, and we expand the 1-D convolution kernel  $h(u)$  at the detector domain to include the virtual depth information in the Fourier space i.e.  $H(f_u, f_w)$ . Since, unfortunately, the impulse response function for projection/backprojection is not available in an analytically closed form, we assume the parallel-beam geometry. This assumption may introduce additional artifacts in the reconstructed images. However, Lauritsch and Härer showed a demonstration of dental images, obtained for the circular tomosynthesis trajectory, with a striking improvement in image quality [7].

For the frequency range,  $|f_w| \leq |f_u| \tan\left(\frac{\beta_{\text{scan}}}{2}\right)$ , in the limited isocentric trajectory, the impulse response is assumed to be [8]

$$\left[ 2 \tan\left(\frac{\beta_{\text{scan}}}{2}\right) |f_u| \sqrt{1 + \left(\frac{f_w}{f_u}\right)^2} \right]^{-1}. \quad (3)$$

Then, the filter is designed as the multiplication of ramp, spectral apodization, and slice thickness filters:

$$H(f_u, f_w) = H_{\text{RA}}(f_u) H_{\text{SA}}(f_u) H_{\text{ST}}(f_w), \quad (4)$$

where

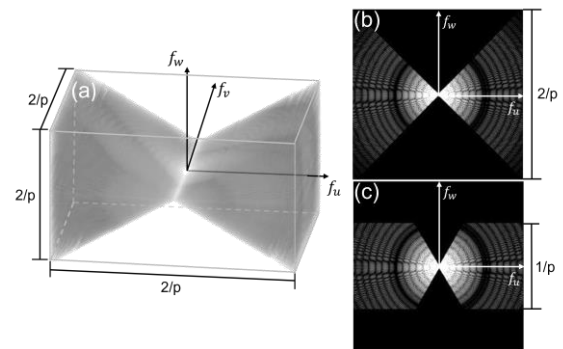


Fig. 1. The Fourier data for an impulse signal obtained from  $\beta_{\text{scan}} = 90^\circ$ : (a) 3D representation of the Fourier data without depth filtering in the Cartesian coordinates. 2D representation of the Fourier data (b) without depth filtering and (c) with depth filtering.  $p$  represents the pixel pitch of a virtual detector.

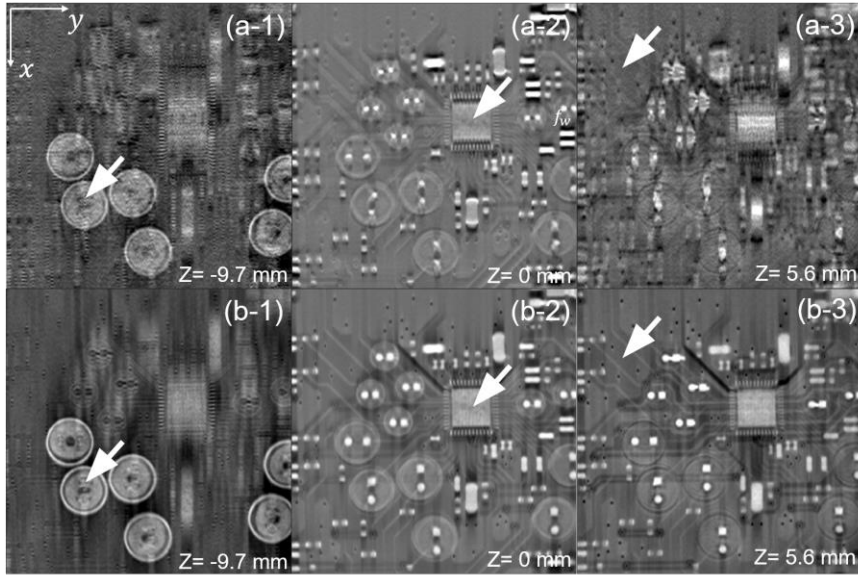


Fig. 2. Comparison of slice images of a PCB sample reconstructed with (a) the conventional algorithm and (b) the proposed algorithm. The depth positions of slice images relative to the axis of rotation are indicated at each image. Arrow shown in each image designates a representative part that shown at the depth: (1) capacitors, (2) an IC chip, and (3) copper interconnections.

$$H_{RA}(f_u) = 2 \tan\left(\frac{\beta_{scan}}{2}\right) |f_u|, \quad (5)$$

$$H_{SA}(f_u) = \frac{1}{2} \left[ 1 + \cos\left(\frac{2\pi f_u}{B_u}\right) \right], \quad (6)$$

$$H_{ST}(f_w) = \frac{1}{2} \left[ 1 + \cos\left(\frac{2\pi f_w}{B_w}\right) \right]. \quad (7)$$

Assuming the detector pixel size as  $p$ , the filter bandwidths are  $B_u = 1/(2p)$  and  $B_w = \tan(\frac{\beta_{scan}}{2}) / (2p)$ .

## 2.2 Experimental

Printed circuit boards (PCBs) were scanned using a bench-top CBCT system. The detector (Shado-o-Box 1548 HS, Teledyne Rad-Icon Imaging Corp., Sunnyvale, CA) features a pixel ( $p = 0.099$  mm) arranged in a  $1032 \times 1548$  format. The x-ray source (Series 5000 XTF5011, Oxford Instruments, US) employs a tungsten target to produce x-ray spectra with energies ranging up to 50 kVp at 50 Watts. The scanning conditions are: the irradiation energy per projection = 45 kVp  $\times$  0.9 mA  $\times$  275 ms;  $d = 443.91$  mm;  $D = 665.86$  mm, and the step angle  $\Delta\beta = 1^\circ$ .

## 3. Preliminary Results

To investigate the effect of depth filtering using the slice-thickness filter, the Fourier data for an impulse signal (i.e. a tiny sphere) were simulated. Figure 1 shows the Fourier data space for the impulse signal obtained for  $\beta_{scan} = 90^\circ$ . The fractional volume of null space is largely decreased when the depth filtering is applied.

Figure 2 compares the slice images at various depth positions of a PCB sample obtained without and with depth filtering in the Feldkamp algorithm. Angular parameters are  $\beta_{scan} = 40^\circ$  and  $\Delta\beta = 2^\circ$ , hence the number of projections used for reconstruction is 21 views. The depth filtering improves the image quality of slice images. Due to the reduced depth resolution in the limited-angle tomography, the out-of-plane blur artifacts are shown in the reconstructed images. For example, at the depth  $z = -9.7$  mm, only the capacitors should be shown. However, as shown in Fig. 2(b-1), the parts distant away are appeared.

## 4. Conclusion

For the CB limited-angle tomography application, we have added a low-pass filter along the depth direction to restrict the high spatial-frequency contents. This filtration is intended to reduce the null space in the Fourier data space, which is unavoidable in the limited-angle tomography while sacrificing the depth resolution. The demonstration of reconstruction images for PCB samples shows a large improvement in image quality compared to the conventional tomographic images. The developed CB limited-angle tomography will be useful for the defect inspection of the objects having thin-slab geometries, such as PCB. More detailed experimental results, including the simulation results, will be presented in the conference with discussions on the effect of the bandwidth of slice-thickness filter on the quality of reconstructed images.

## ACKNOWLEDGEMENTS

This work was supported by the National Research Foundation of Korea (NRF) grant funded by the Korea government (MSIP) (No. 2021R1A2C1010161).

## **REFERENCES**

- [1] M. K. Cho, H. Youn, S. Y. Jang, and H. K. Kim, Cone-Beam Digital Tomosynthesis for Thin Slab Objects, *NDT&E International*, Vol. 47, pp. 171-176, 2012.
- [2] N. S. O'Brien, R. P. Boardman, I. Sinclair, and T. Blumensath, Recent Advances in X-Ray Cone-Beam Computed Laminography, *Journal of X-Ray Science and Technology*, Vol. 24, pp. 691-707, 2016.
- [3] D. Kim, D. W. Kim, J. Yon, S. Ha, S. H. Kim, H. Youn, and H. K. Kim, Spatial Resolution and Blurring Artifacts in Digital X-Ray Tomosynthesis, *IEEE Transactions on Nuclear Science*, Vol. 65, pp. 1180-1186, 2018.
- [4] K. M. Hanson, Computed Tomographic (CT) reconstruction from limited projection angles, *Proc. SPIE*, Vol. 347, pp. 166-173, 1982.
- [5] H. E. Knutsson, P. Edholm, G. H. Granlund, and C. U. Petersson, Ectomography—A New Radiographic Reconstruction Method—I. Theory and Error Estimates, *IEEE Transactions on Biomedical Engineering*, Vol. BME-27, pp. 640-648, 1980.
- [6] L. A. Feldkamp, L. C. Davis, and J. W. Kress, Practical Cone-Beam Algorithm, *Journal of the Optical Society of America A*, Vol. 1, pp. 612-619, 1984.
- [7] G. Lauritsch and W. H. Härer, A Theoretical Framework for Filtered Backprojection in Tomosynthesis, *Proc. SPIE*, Vol. 3338, pp. 1127-1137, 1998.
- [8] T. Mertelmeier, J. Orman, W. Haerer, and M. K. Dudam, Optimizing Filtered Backprojection Reconstruction for a Breast Tomosynthesis Prototype Device, *Proc. SPIE*, Vol. 6142, p. 61420F, 2006.